

## htof: A new open-source tool for analyzing Hipparcos, Gaia, and future astrometric missions.

G. MIREK BRANDT <sup>1,\*</sup> DANIEL MICHALIK <sup>2,†</sup> TIMOTHY D. BRANDT <sup>1</sup> YITING LI <sup>1</sup> TRENT J. DUPUY <sup>3</sup> AND YUNLIN ZENG<sup>1,4</sup>

<sup>1</sup>*Department of Physics, University of California, Santa Barbara, Santa Barbara, CA 93106, USA*

<sup>2</sup>*European Space Agency (ESA), European Space Research and Technology Centre (ESTEC), Keplerlaan 1, 2201 AZ Noordwijk, The Netherlands*

<sup>3</sup>*Institute for Astronomy, University of Edinburgh, Royal Observatory, Blackford Hill, Edinburgh, EH9 3HJ, UK*

<sup>4</sup>*School of Physics, Georgia Institute of Technology, 837 State Street, Atlanta, Georgia, USA*

(Accepted July 7, 2021)

Submitted to AJ

### ABSTRACT

We present **htof**, an open-source tool for interpreting and fitting the intermediate astrometric data (IAD) from both the 1997 and 2007 reductions of *Hipparcos*, the scanning-law of *Gaia*, and future missions such as the Nancy Grace Roman Space Telescope (*NGRST*). **htof** solves for the astrometric parameters of any system for any arbitrary combination of absolute astrometric missions. In preparation for later *Gaia* data releases, **htof** supports arbitrarily high-order astrometric solutions (e.g. five-, seven-, nine-parameter fits). Using **htof**, we find that the IAD of 6617 sources in *Hipparcos* 2007 might have been affected by a data corruption issue. **htof** integrates an ad-hoc correction that reconciles the IAD of these sources with their published catalog solutions. We developed **htof** to study masses and orbital parameters of sub-stellar companions, and we outline its implementation in one orbit fitting code (**orvara**). We use **htof** to predict a range of hypothetical additional planets in the  $\beta$  Pic system, which could be detected by coupling *NGRST* astrometry with *Gaia* and *Hipparcos*. **htof** is pip installable and available at <https://github.com/gmbrandt/htof>.

*Keywords:* —

### 1. INTRODUCTION

Astrometric missions like *Hipparcos* or *Gaia* measure absolute positions, parallaxes, and motions for the stars that they survey (Perryman 2012). These missions observe a star many times and fit a model to that star’s motion in the plane of the sky, also known as the star’s ephemeris. A star’s apparent motion is most simply modeled as parallactic motion (motion induced by the earth’s orbit) together with a constant velocity; encoded in five parameters. The *Hipparcos* (Perryman et al.

1997; van Leeuwen 2007a) and *Gaia* (Gaia Collaboration et al. 2016, 2018a; Lindegren et al. 2018; Gaia Collaboration et al. 2020) catalogs report the five best-fit astrometric parameters: two position parameters at a reference epoch, two proper motions, and the parallax. The five-parameter astrometric model, however, is only an approximation: even a single star with a constant 3D velocity exhibits apparent accelerations when its motion is projected into spherical coordinates (perspective acceleration; Michalik et al. 2014; Lindegren & Dravins 2021). Stars may also accelerate due to visible and/or unseen companions, or even due to their orbits through the Galaxy.

The influence of unseen companions may be modeled as a higher-order astrometric fit with seven or nine parameters, or as a full Keplerian orbit. The first full orbital fits of *Hipparcos* astrometry were done by the *Hip*

Corresponding author: G. Mirek Brandt  
[gmbrandt@physics.ucsb.edu](mailto:gmbrandt@physics.ucsb.edu)

\* NSF Graduate Research Fellow

† ESA Research Fellow

*parcos* team themselves (Lindgren et al. 1997). Work over the following decades built on this work to include brown dwarfs and giant planets (e.g., Zucker & Mazeh 2001; Sozzetti & Desidera 2010; Reffert & Quirrenbach 2011; Sahlmann et al. 2011; Snellen & Brown 2018). The most recent additions to this field are covering harder to detect and less massive exoplanets, leveraging the long-term proper motion anomalies between *Hipparcos* and *Gaia* (Brandt 2018; Brandt et al. 2018; Calissendorff & Janson 2018; Dupuy et al. 2019; Fontanive et al. 2019; Kervella et al. 2019; Feng et al. 2019; Maire et al. 2020; Currie et al. 2020; Brandt et al. 2021a).

For companions with orbital periods  $\lesssim 10$  yr, proper motion accelerations within *Hipparcos* and *Gaia* become important to model. The intermediate astrometric data (hereafter, IAD) of the *Hipparcos* mission—the individual position measurements and uncertainties for every star—are available. The *Gaia* IAD for every star will be unavailable for many years, but the spacecraft’s scanning law—its predicted scan angles and observational epochs as a function of sky position—is available through the *Gaia* Observation Forecast Tool (GOST; Fernández-Hernández & Joliet 2019).<sup>1</sup> Several groups have used GOST predictions to forward model *Gaia* astrometry in the context of orbit fitting (e.g., Brandt et al. 2019; Nielsen et al. 2019; De Rosa et al. 2020).

In this paper, we present a tool, *htof* (Brandt & Michalik 2021), that uses the IAD for *Hipparcos* and the scanning law of *Gaia* to fit sky paths. Although *htof* extends beyond the hundred thousand sources of *Hipparcos*, *htof* stands for the Hundred Thousand Object Fitter in homage to the hundred-thousand-proper-motion project (de Bruijne, J. H. J. & Eilers, A.-C. 2012; Michalik et al. 2014). For both *Gaia* and *Hipparcos*, *htof* can compute fits with arbitrarily many parameters, e.g., five-, seven-, and nine-parameters. Given the *Hipparcos* IAD for a star, *htof* computes likelihoods and parameter errors directly comparable to the catalog values for that star. For *Gaia*, *htof* is currently limited to approximate likelihoods and errors because the actual observations and their uncertainties are not yet available.

*htof*’s capabilities make it well suited for exploring many problems such as simulating the planets which could be discovered by future astrometric missions. The likelihoods computed by *htof* also enable full Keplerian orbital fits if combined with common-reference-frame and cross-calibrated positions and errors from *Hipparcos* and *Gaia*, e.g. from the *Hipparcos-Gaia* Catalog of

Accelerations (Brandt 2018). *htof* was used in a number of papers exploiting the latter technique for studying dynamical masses and orbital parameters of sub-stellar companions in nearby stellar systems (Brandt et al. 2019; Brandt et al. 2021a; Bowler et al. 2021a,b).

This paper is structured as follows. In Section 2, we describe *Gaia*, *Hipparcos*, fitting astrometry, and parsing the IAD. In Section 3, we discuss *htof* along with its implementation, validation, and limitations.

In Section 4, we discuss a suspected data corruption affecting 6617 sources in the *Hipparcos* 2007 IAD. We have developed an ad-hoc correction algorithm to recover their best-fit residuals. It is readily integrated in *htof*. We then discuss two major use cases. We outline *htof*’s utility in orbit fitting in Section 5. In Section 6, we demonstrate how *htof* can predict what new planets could be discovered by combining *Gaia* astrometry with measurements from the Nancy Grace Roman Space Telescope (*NGRST*) (Spergel et al. 2015). We summarize our results in Section 7.

## 2. OBSERVING AND FITTING AN ASTROMETRIC SKY PATH

*Gaia* and *Hipparcos* observe stars by scanning the sky in a repetitive pattern, called the scanning law (van Leeuwen & Evans 1998; *Gaia* Collaboration et al. 2016). For both satellites, the continuous scans along overlapping great circles mean that each observation is precise in the direction along the scan (along-scan; AL), and imprecise perpendicular to the scan (across-scan; AC). This renders each observation effectively one-dimensional (*Gaia* Collaboration et al. 2016).

Figure 1 shows the definitions we use for the scan-angle  $\theta$  of the observation and the abscissa residual, consistent with the definitions given in *Gaia* Collaboration et al. (2018b) and online.<sup>2</sup> The scan angle  $\psi$  of the 2007 *Hipparcos* re-reduction is defined differently than for *Gaia*, but this is handled by a conversion discussed in Section 2.2.2. In Figure 1, the spacecraft spin direction is indicated by the AL arrow, the spin axis is perpendicular to it in the AC direction. The (essentially one-dimensional) error-ellipse of an observation is indicated by the red double-headed arrow. *Hipparcos* and *Gaia* fit sky paths to the abscissa residuals; the model sky paths are collectively referred to as *the astrometric solution*. The shortest distance between the prediction of the best-fit astrometric model at the observational epoch and the 1-d observed position is called the abscissa residual  $\nu$ .

<sup>1</sup> <https://gaia.esac.esa.int/gost/>

<sup>2</sup> <https://www.cosmos.esa.int/web/gaia/scanning-law-pointings>

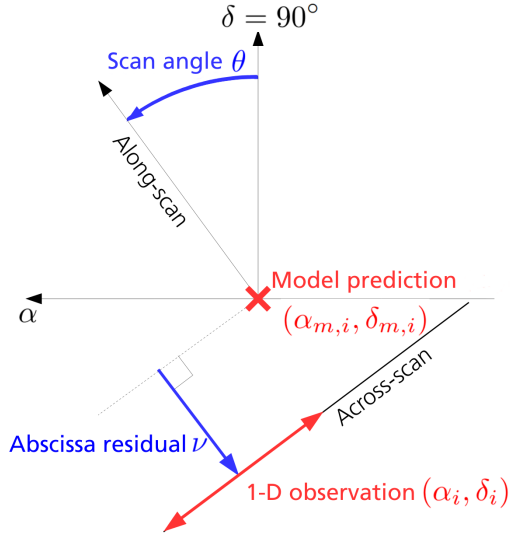


**Figure 1.** Definition of the scan angle  $\theta$  and the abscissa residual  $\nu$  between the one-dimensional observation  $(\alpha_i, \delta_i)$  and the best-fit astrometric model  $(\alpha_{m,i}, \delta_{m,i})$ .

The astrometric solution for a given star is the set of model parameters that minimizes the sum of the squared AL abscissa residuals weighted by the inverse of the AL variances. A good astrometric solution requires data with good geometric and temporal coverage, i.e., many different scan angles at many different epochs. In the following subsections, we discuss how to obtain the best-fit astrometric parameters from the IAD.

### 2.1. Fitting the Sky Path

For a five-parameter astrometric model, the observed position on the sky is the sum of the parallax, proper motion, and position multiplied by known functions of time. Higher order models include acceleration and jerk terms. Fitting the ephemerides under 5, 7, or 9-parameter models is a linear problem, and may be solved by minimizing the chi-squared of the abscissae with respect to the astrometric parameters. The chi-squared minimization problem can be transformed into a matrix equation which can then be solved by any standard linear algebra method, e.g., singular value decomposition in `htof`. The model for the star's motion across the sky that we adopt is

$$\begin{aligned}\alpha_{m,i} &= \varpi f_{\varpi}[t_i] + \sum_{n=0}^N \frac{a_n}{n!} (t_i - t_{\text{ref}})^n \\ \delta_{m,i} &= \varpi g_{\varpi}[t_i] + \sum_{n=0}^N \frac{b_n}{n!} (t_i - t_{\text{ref}})^n\end{aligned}\quad (1)$$

where  $(\delta_{m,i}, \alpha_{m,i})$  is the predicted model declination and right-ascension at time  $t_i$ .  $a_n, b_n$  are the astrometric parameters excluding parallax (e.g.  $b_1 = \mu_{\delta}$ ),  $N$  is the

degree of the fit ( $N = 1$  for a five-parameter fit),  $\varpi$  is the parallax angle, and  $f_{\varpi}[t_i], g_{\varpi}[t_i]$  are the parallax factors (van Leeuwen 2007b). These are the perturbations in declination and right-ascension, respectively, due to parallax alone for a parallax angle of unity.  $f_{\varpi}[t_i] \cos(\theta_{\text{scan}}) + g_{\varpi}[t_i] \sin(\theta_{\text{scan}})$  is equal to  $\frac{\partial r_i}{\partial \varpi}$ , the derivative of the residual with respect to parallax. We use modules from `astrometric-sky-path`<sup>3</sup> to compute the parallax factors.

The *Hipparcos* catalog abscissa residuals  $\nu_i$  are with respect to the along-scan direction only (for both the 1997 and 2007 catalogs). The matrix equation can be constructed, and in turn the best-fit astrometric parameters can be solved for, purely in terms of the along-scan derivatives and abscissa residuals (Perryman et al. 1997). Alternatively, one can first cast the measurements into the equatorial coordinate system and construct the matrix equation from those right-ascension and declination observations. The former approach is closer to how the *Hipparcos* team handled the data (Perryman et al. 1997), while `htof` uses the latter approach, whereby we minimize Equation (2). The two are equivalent, but we employ the latter because then the input data are more familiar: right ascension and declination instead of along-scan abscissa residuals and derivatives.

We therefore assume that we have: the covariance matrix  $C_i$  for an observation  $i$  which occurred at epoch  $t_i$  and the corresponding right-ascension  $\alpha_i$  and declination  $\delta_i$ . We obtain the  $\delta_i, \alpha_i$  by decomposing each abscissa residual  $\nu_i$  into the two equatorial components. We find the best-fit astrometric parameters by minimizing

$$\chi^2 = \sum_i \begin{pmatrix} \alpha_{m,i} - \alpha_i & \delta_{m,i} - \delta_i \end{pmatrix} C_i^{-1} \begin{pmatrix} \alpha_{m,i} - \alpha_i \\ \delta_{m,i} - \delta_i \end{pmatrix}, \quad (2)$$

In detail, the parallactic motion of any object with a non-zero proper motion will change as it moves through the sky. The parallax factors are functions of position as well as time. Nonlinear effects such as perspective acceleration are negligible for most stars. For example, Lindegren et al. (2018) lists only 53 stars where nonlinear effects warrant correction, one of which is Barnard's star ( $\mu \approx 10'' \text{ yr}^{-1}$ ; van de Kamp 1935; Luyten 1979). We therefore always assume that the model (Equation 1) is linear.

We solve for the best-fit parameters by taking the partial derivative of Equation (2) with respect to each of the free parameters. The partials yield a matrix equation of

<sup>3</sup> <https://github.com/agabrown/astrometric-sky-path>

full rank (e.g., a  $9 \times 9$  matrix if  $N = 3$  in Eq. 2) which is linear in every parameter. We solve for the best-fit parameters with singular value decomposition.

## 2.2. Obtaining astrometry from *Hipparcos* IAD and the *Gaia* scanning law

To recover a solution for each source we need the epochs of observation, the source’s position in the sky at each epoch, and the covariance matrix of the observation at each epoch. In this section, we detail how to obtain and parse those quantities from *Hipparcos* and *Gaia*.

For both *Hipparcos* reductions, the IAD are enough to calculate full positions and covariance matrices. For *Gaia*, we use the predicted scanning law as a proxy for the IAD. We calculate positions assuming the *Gaia* catalog astrometric parameters, and calculate the epochs and covariance matrices for each observation.

Table 1 summarizes how to extract the scan angles, observation times and along-scan errors from the IAD from both *Hipparcos* reductions and the *Gaia* scanning law. Each variable and column in Table 1 is named in accordance with each astrometry product. We now turn to details of the IAD and the scanning law.

### 2.2.1. The original (1997) *Hipparcos* catalog

The IAD for the original *Hipparcos* catalog (Perryman et al. 1997) are available from the Strasbourg Astronomical Data Center (CDS) FTP archive.<sup>4</sup> The IAD give the scan angles, abscissa residuals relative to the first five parameters of the best-fit sky path, formal AL errors for each observation, and time of observation. Each file from the IAD has ten columns, referred to in the documentation as IA1 through IA10. In the second column (IA2), each row is labelled either N or F for NDAC for FAST, depending on which consortium reduced the data. The formal AL errors ( $\sigma_{AL}$ ) are in column IA9 and the abscissa residuals are given in column IA8. The scan angle is  $\arctan2(\text{IA3}, \text{IA4})$  (van Leeuwen & Evans 1998).

The astrometric parameters in the original *Hipparcos* catalog are those which best-fit the merged IAD. We merge the NDAC and FAST IAD following the procedure described by the *Hipparcos* team (see Section 3.2 of van Leeuwen & Evans 1998). For each epoch that contains both NDAC and FAST data, we average the values from both consortia weighted by Best-Linear-Unbiased-

Estimator (BLUE) weights. These weights, a pair per epoch, are determined uniquely by the covariance matrix constructed according to Equation 7.11 on page 377 of Volume 3 of Perryman et al. (1997), using the NDAC-FAST correlation coefficient in column IA10. We exclude observations rejected from the *Hipparcos* merged solution (Perryman et al. 1997), which are designated by a lowercase letter in the consortium designation.

### 2.2.2. The 2007 re-reduction of the *Hipparcos* data

Ten years after the publication of the original *Hipparcos* catalog, van Leeuwen (2007a) re-reduced the raw data to produce new astrometric fits. At the time of writing, there are three sets of the *Hipparcos* re-reduction catalog. First, and oldest, is the Digital Versatile Disc (DVD) included with van Leeuwen (2007a), which contains the first published version of the catalog as well as the IAD used to construct it. Second is the Vizier catalog,<sup>5</sup> which does not include the IAD. Third, and most recent, is the data distributed with a Java tool.<sup>6</sup> This tool includes the IAD but not in per-source human readable data files as are on the DVD. We have extracted the IAD from the Java tool (van Leeuwen & Michalik 2019, private comm.); a copy of the dataset is available at <https://www.cosmos.esa.int/web/hipparcos/hipparcos-2>. All three sources give data which are similar for every star, yet not identical. One must consistently use the IAD together with the catalog it accompanied. For example, one should not mix catalog values from Vizier with the IAD from the DVD. For most sources, results using the IAD from the DVD are indistinguishable from results using the IAD from the Java tool. One advantage of the Java tool data is that rejected transits are clearly denoted by negative AL errors. Rejected observations are not designated in the DVD IAD.

The columns of the residual records of the 2007 IAD (both the DVD and Java tool) are defined in Table G.8 of van Leeuwen (2007b). The fourth column gives  $\cos(\Psi) = \sin(\theta)$ , and the fifth column gives  $\sin(\Psi) = \cos(\theta)$ , where  $\theta$  is the scan angle and  $\Psi = \pi/2 - \theta$ . We index the first column as 1 to be consistent with the original reduction’s documentation. The AL errors are given in column 7 for the re-reduction. The abscissa residuals are in column 6. For sources with 7 and 9 parameter solutions, the residuals in the *Hipparcos* 2007 IAD are relative to the full 7 or 9 parameter solutions. This is in contrast to *Hipparcos* 1997 where the resid-

<sup>4</sup> [http://cdsarc.u-strasbg.fr/ftp/1/239/version\\_cd/cats/hip\\_i.dat.gz](http://cdsarc.u-strasbg.fr/ftp/1/239/version_cd/cats/hip_i.dat.gz)

<sup>5</sup> <http://vizier.u-strasbg.fr/viz-bin/VizieR?-source=I/311>

<sup>6</sup> <https://www.cosmos.esa.int/web/hipparcos/interactive-data-access>



**Table 1.** Summary of extracting the scan angles, epochs, residuals, and along-scan errors ( $\sigma_{AL}$ ) from the three catalogs.

Reduction	Scan angle (radian)	Epoch	$\sigma_{AL}$	AL residuals	Reference <sup>1</sup>
Hip 1	$\arctan2(\text{IA3}, \text{IA4})$	$J1991.25 + \frac{\text{IA6}}{\text{IA3}}$ OR $J1991.25 + \frac{\text{IA7}}{\text{IA4}}$	<b>IA9</b>	<b>IA8</b>	vLE98
Hip 2 DVD	$\arctan2(\text{Column 4}, \text{Column 5})$	Column 2 + $J1991.25$	Column 7	Column 6	vL07
Gaia DR2	<b>scanAngle</b>	<b>ObservationTimeAtBarycentre</b>	...	...	FHJ19

NOTE—Hip 1 refers to the 1997 reduction (Perryman et al. 1997), and Hip 2 to the 2007 re-reduction (van Leeuwen 2007a).

<sup>1</sup>References abbreviated as vLE98 (van Leeuwen & Evans 1998), vL07 (van Leeuwen 2007b, Table G.8), and FHJ19 (Fernández-Hernández & Joliet 2019).

uals are defined with respect to the skypath described by only the first five parameters, regardless of solution type.

### 2.2.3. The Gaia Observation Forecast Tool (GOST)

Gaia Data Release 1 (DR1), DR2, and EDR3 (Gaia Collaboration et al. 2016, 2018a; Lindegren et al. 2018; Gaia Collaboration et al. 2020) contain model parameters (positions, proper motions, parallaxes, and their uncertainties and covariances), but neither the epoch astrometry, the along-scan residuals, nor the per-epoch covariance matrices. The full epoch astrometry will be released in the final catalog of the nominal mission.<sup>7</sup> **htof** uses GOST as a stand-in for these data. GOST provides predicted observations and scan angles for any Gaia source. The GOST data should be downloaded manually as a .csv (see the `readme` with the **htof** source code), but a future version of **htof** may automate this. **htof** places the GOST data into a suitable form for fitting as if they were the Gaia IAD. GOST-predicted scans, parsed by **htof**, are used in a variety of orbital analyses of brown dwarf companions to help constrain companion masses and orbital inclinations. For instance Brandt et al. (2019); Brandt et al. (2021a); Bowler et al. (2021a,b). However, there are important details to consider with the planned observations.

Not all of the planned observations will be used in the astrometric solution. Some predicted scans will represent missed observations (satellite dead times), executed but unusable observations (e.g., from cool-down after decontamination), or observations rejected as astrometric outliers. Rejected observations could be corrupted due to, e.g., micro-clanks, scattered light from a nearby bright source, crowded fields, micro-meteoroid hits, etc.<sup>8</sup> Such problematic observations do not constrain the Gaia astrometric solution. In practice, up to 20% of Gaia ob-

servations predicted by GOST are excluded from the analysis that produced DR2 (ESA accessed February 4, 2020). The largest stretches of dead times and rejected observations are published as astrometric gaps. **htof** accounts for the published astrometric gaps for DR2.<sup>9</sup> and EDR3 (Table 1 of Lindegren et al. 2020).

### 2.3. Constructing the covariance matrix for each observation

We need the inverse covariance matrix for every observation,  $\mathcal{C}_i^{-1}$ , to evaluate and minimize  $\chi^2$  (Equation 2). We construct  $\mathcal{C}_i^{-1}$  from the scanning law or the IAD. We define the ratio of the AC to AL variances as  $r$  and assume these two measurements to be independent. By default, **htof** has  $r = \infty$  because *Hipparcos* and *Gaia* both optimize for AL. For *Hipparcos*, we have the individual AL uncertainties for all observations. For *Gaia*, we do not and so we assume the AL error to be the same for all epochs of a given source. The covariance matrix at each epoch is then correct up to a (unknown) constant (the along-scan error).<sup>10</sup>

Given a scan angle  $\theta_i$ ,  $r$ , and AL error  $\sigma_{AL,i}$ , for the  $i^{\text{th}}$  observation, we construct the covariance matrix  $\mathcal{C}_i$  by rotating the covariance matrix in the scan basis into the equatorial coordinate system as follows.

$$\mathcal{C}_i = \sigma_{AL,i}^2 R(\theta_i) \begin{pmatrix} 1 & 0 \\ 0 & r \end{pmatrix} R^T(\theta_i) \quad (3)$$

$$\text{where } R(\theta_i) = \begin{pmatrix} \sin \theta_i & -\cos \theta_i \\ \cos \theta_i & \sin \theta_i \end{pmatrix}$$

In Eq. (3),  $R(\theta)$  is the inverse of the transformation matrix in Eq. (3) of Gaia Collaboration et al. (2018b) and  $R^T(\theta)$  its transpose. For *Gaia*, we assume uniform

<sup>7</sup> <https://www.cosmos.esa.int/web/Gaia/release>

<sup>8</sup> <https://www.cosmos.esa.int/web/gaia/dr2-data-gaps>

<sup>9</sup> See footnote 8

<sup>10</sup> See section 6.1.1 of Brandt et al. (2021c) for a discussion of the limitation of the uniform AL error assumption in the context of Gl 229.

AL errors and set  $\sigma_{AL}^2$  to unity for every observation of a given source. We multiply each *Hipparcos* re-reduction  $\sigma_{AL}$  by the scaling factor  $u$  in Equation B.4. of Michalik et al. (2014). This is a renormalization to match van Leeuwen (2007b), where the errors were normalized such that the reduced  $\chi^2$  of the fit was unity. The inverse covariance matrix is

$$\mathcal{C}_i^{-1} = \frac{1}{\sigma_{AL,i}^2} R(\theta_i) \begin{pmatrix} 1 & 0 \\ 0 & 1/r \end{pmatrix} R^T(\theta_i) \quad (4)$$

where  $1/r = 0$  for *Hipparcos* and by default in `htof`. With the inverse covariance matrix for each observed right-ascension  $\alpha_i$  and declination  $\delta_i$ , we generate the astrometric model which best fits those observations according to Section 2.1.

### 3. `htof`

`htof` is an open-source *Python* package available at <https://github.com/gmbrandt/htof> which parses and fits astrometric data according to the methods discussed in Section 2.

#### 3.1. User guide and core features

`htof` is designed to fit 5-, 7-, and 9-parameter models to any *Hipparcos* or *Gaia* source. It can calculate the full covariance matrix of the fit, calculate central epochs of observation, perform an ad-hoc correction of the 2007 IAD for 6617 sources (Section 4), and combine astrometric missions (useful for forecasting; Section 6). It possesses a variety of other minor features. `htof` does not provide an automated download (as of version 1.0.0) of the *Hipparcos* IAD (either reduction) or *Gaia* GOST data. These data must be downloaded manually.

`htof` can analyze data from arbitrary astrometric missions. `htof` is centered around `DataParser` subclasses which parse the IAD or scanning law into scan angles, errors, etc., and a single `AstrometricFitter` class which generates an astrometric solution from data within any of the numerous `DataParser` subclasses. The `DataParser` classes hold the data in a consistent way so that the single fitter class, `AstrometricFitter`, can fit an astrometric sky path. There is also a convenience `Astrometry` class, which wraps all the functionality of the data parser and fitting classes. For examples of fits and other functionality, we refer the reader to the documentation `readme` and the *Jupyter* example notebook that is packaged with the source code. In the following, we review `htof`’s core functionality of astrometric fitting.

`Astrometry.fit(ra, dec)` returns an array of the best-fit astrometric parameters. If the fit degree is 1 and `Astrometry` is instantiated with `use_parallax=True`,

this array will be  $(\varpi, \alpha_0, \delta_0, \mu_{\alpha*}, \mu_{\delta})$ : the parallax angle, the right-ascension and declination (relative to the reference right-ascension and declination provided to `Astrometry()`), the proper motion in right-ascension, and the proper motion in declination — by default with units of mas and  $\text{mas yr}^{-1}$ . If `fit(ra, dec, return_all=True)` is used, then the fit will return the best-fit parameter array, an array of the standard errors of each parameter, and the formal chi-square of the fit. The `AstrometricFitter` can provide the full covariance matrix if it is desired (not just the errors on each parameter), examples of this are in the *Jupyter* notebook with the source code.

Fitting requires providing a reference epoch around which to center the observations. For *Hipparcos* 1997 catalog solutions, the consortia used J1991.25. The choice of reference epoch will affect the values, errors, and covariances for all but the highest-order terms in any fit. For example, changing the reference epoch for a five-parameter fit will affect the fitted reference positions, their errors and covariances, but not the proper motions. Choosing a reference epoch far away from the optimal epoch (e.g., choosing the year 1000 for *Hipparcos* instead of 1991.25) will result in numerical instability and a poorly constrained solution.

#### 3.2. Validation of the fits to the *Hipparcos* IAD

`htof` can reproduce the catalog solutions for the vast majority of sources in both *Hipparcos* reductions from the IAD. At the time of this publication, `htof` is designed for sources with 5, 7, or 9-parameter solutions, from both *Hipparcos* reductions. Future versions of `htof` may incorporate sources with VIM (V), stochastic (X), component (C), or orbital (O) solutions. We point the reader to the `readme` with the source code for the up-to-date capabilities of the code.

In the current version (1.0.0), there is a subset of the *Hipparcos* five-, seven-, and nine-parameter sources for which the best-fit `htof` parameters disagree slightly with the catalog values. For the vast majority of sources, `htof` matches the catalog values either exactly after rounding, or with a scatter that is attributable to round-off within the intermediate astrometric data. We found that offsets up to  $\pm 0.01 \text{ mas yr}^{-1}$  in both right-ascension or declination could be attributed to round off based on Monte-Carlo simulations of randomly selected disagreeing sources. There are only a small number of sources that `htof` cannot fit well: 120 sources disagree more than  $0.1 \text{ mas yr}^{-1}$  in proper motion in either direction. We label these 120 sources as “flagged” and provide a list of them in the file `htof/data/hip1_flagged.txt`. A  $0.1 \text{ mas yr}^{-1}$  disagreement is typically less than  $1/2$

of a standard error for the discrepant sources. The fraction of discrepant sources is similar for the *Hipparcos* 2007 re-reduction, but only after applying our proposed ad-hoc correction to the IAD.

#### 4. AD-HOC CORRECTION TO 6617 SOURCES IN HIPPARCOS 2007

*Hipparcos* 2007 was a momentous effort largely by one individual. It is and remains an invaluable record of stellar astrometry. As with every data set, deeper analysis sometimes reveals new ways of interpreting the data. Here we propose an improvement to the *Hipparcos* 2007 IAD.

We found 6617 sources from *Hipparcos* 2007 for which the astrometric solution implied by the IAD is significantly discrepant with the published catalog parameters. Two examples are HIP 651 and 44050. Discrepant sources are present both in the Java tool and in the DVD IAD. The subset of discrepant sources is almost, but not exactly, identical between the two. However, we limit our discussion of the issue and our ad-hoc correction to the IAD from the Java tool. The Java tool includes a clear designation of rejected transits. Without knowing the regularly rejected transits, our ad-hoc correction algorithm becomes combinatorially unfeasible. There is ongoing work to understand these 6617 sources in more detail (van Leeuwen & Michalik, D 2021, private comm.).

To identify the issue, we first read in the IAD for every *Hipparcos* source. We compute the partial derivatives of  $\chi^2$  with respect to each of the astrometric parameters, normalized by the standard errors to make them dimensionless (e.g.,  $\sigma_{\mu\alpha} \frac{\partial \chi^2}{\partial \mu_\alpha}$ ). If the residuals from the IAD correspond to a solution that minimizes  $\chi^2$ , then these partials will all be zero within round-off error. For most sources, the quadrature sums of the scaled partial derivatives are indeed nearly zero, ranging from  $10^{-2}$  to  $10^{-7}$ . For the 6617 sources that we cannot refit, these partial derivative sums are significantly non-zero (e.g.,  $> 1$ ) – implying that the best-fit residuals (data minus model) listed in the IAD are not the residuals with respect to the model that minimizes  $\chi^2$ . As another check, we also refit the IAD with the appropriate astrometric model (5, 7, or 9-parameters) and compare the refit proper motions to those in the catalog. The refit proper motions do not match the catalog values for the discrepant sources.

The top panel of Figure 2 displays the quadrature sum of the chi-squared partials for all five-parameter sources, along with the difference between our refit proper motion and the catalog proper motions. The 6617 sources (colored in red) form a clear outlier cloud.

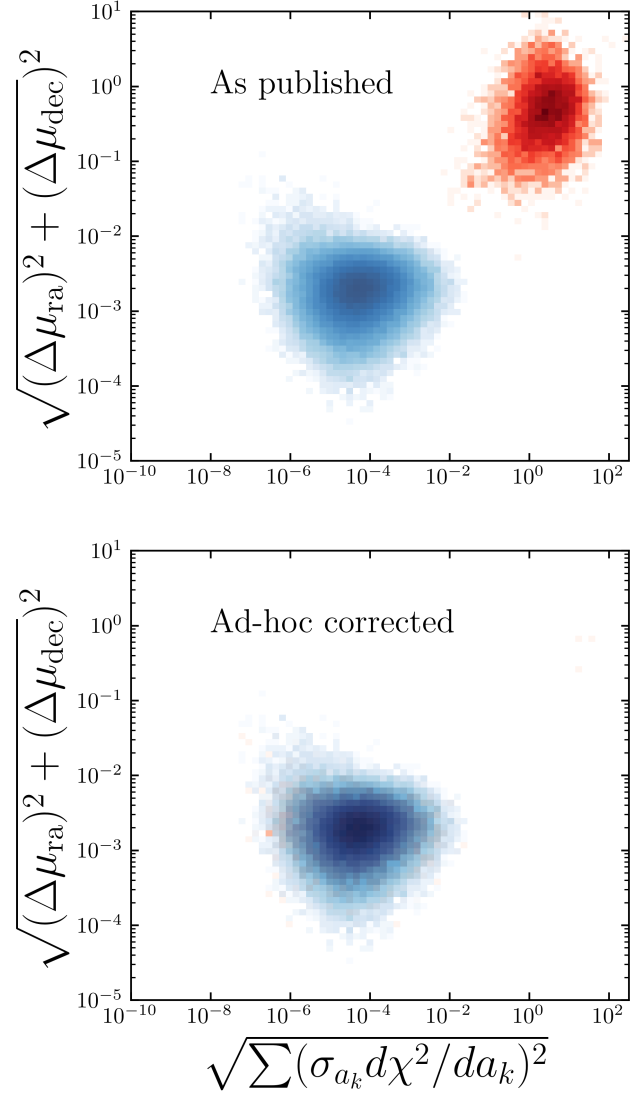


**Figure 2.** Distributions of the proper motion difference and quadrature sums of partial derivatives of fits to the *Hipparcos* Java tool IAD before (top panel) and after (bottom panel) the *htof* IAD ad-hoc correction. All 115,100 five-parameter sources are shown. The vertical axis shows the quadrature sum of the proper motion discrepancies (difference between the catalog values and the values obtained by refitting the IAD). The horizontal axis shows the five partial derivatives of chi-squared ( $\chi^2$ ) also added in quadrature:  $\sqrt{(\sigma_{\varpi} \partial \chi^2 / \partial \varpi)^2 + (\sigma_{\mu\alpha} \partial \chi^2 / \partial \mu_\alpha)^2 + \dots}$ . The 6617 sources with a suspected IAD corruption are colored red, otherwise sources are blue. Upper panel: The results of the refit without *htof*’s ad-hoc correction. Lower panel: All five-parameter sources, after our ad-hoc correction. All of the former outliers that we applied our algorithm to (all but 38) are now well-behaved and a fit of their IAD yields the catalog solution (blue and red data points overlap).

The culprit of the non-reproducibility of these 6617 sources appears to be data corruption in the IAD. Al-

most all of the discrepant sources have one or more lines of repeating AL errors at the end of their IAD file. The number of repeats,  $n$ , varies from source to source. For example, HIP 12241 has as the last four along-scan errors (in mas): 4.92, 4.10, 4.92, and 4.10. For HIP 42975 and 21000, the last ten along-scan errors are repeated in the same sequence. A second clue comes from the IAD header, which states the number of observations considered for the astrometric solution of a given source. For the problematic sources this number is  $n$  less than the number of residual records available in the IAD file. This discrepancy persists even after removing transits marked as rejected by negative AL errors. An example is HIP 651, where the IAD header states 164 observations considered, but the residual records contain 165 transits. The mismatch between observations considered and residuals available is 1 for 5919 of these 6617 sources, 419 have  $n = 2$ .

Deleting the last  $n$  rows does not resolve the issue. We suspect instead that an additional  $n$  transits were supposed to be removed at some stage of the astrometric processing, but were accidentally only partially removed: we suggest that these  $n$  transits were removed from the data structures holding columns 6 and 7 of the IAD, but accidentally kept in the data structures corresponding to the first five columns. The repeating values of AL errors we observe could then be explained by access beyond the memory allocated for columns 6 and 7. Following this assumption, we developed an ad-hoc correction algorithm. This algorithm is described in detail in Appendix A.

The lower panel of Figure 2 shows the new distribution of proper motion discrepancies and  $\chi^2$  values after applying our ad-hoc correction algorithm to the IAD. The entire outlier cloud is removed, except for 38 sources where the ad-hoc correction is combinatorially infeasible. Refitting the modified IAD always recovers the catalog parameters. This strongly supports that our algorithm is correct and that the 6617 outliers that we discovered were caused by data corruption in their IAD.

We do not apply our ad-hoc correction to 38 sources because  $n$  is so great for these sources that our ad-hoc correction requires an inordinately large computation time. GJ 660 (HIP 84123) is among these 38, which has  $n = 21$  (which would take roughly 200 days on a single CPU core to correct). A list of the 38 outliers that we do not correct are listed in `htof/data/hip2.Javatool_flagged.txt`. `htof` applies the ad-hoc correction automatically to any IAD from the Java tool, except these 38 sources.

This fix is important for many uses of the IAD. Many *Hipparcos* sources host planetary or brown dwarf com-

panions, and the masses of these companions can be measured by fitting the proper motion anomalies derived from five-parameter fits to the IAD (e.g., Brandt et al. 2018; Venner et al. 2021). Alternatively, many authors have fit the positions from the *Hipparcos* 2007 IAD directly in orbital analyses (e.g., Sahlmann et al. 2011; Quirrenbach et al. 2011; Snellen & Brown 2018; Feng et al. 2019; Nielsen et al. 2019; Lagrange et al. 2020). Future studies may include some of the 6617 sources. Without a correction of the data, the recovered proper motions can be systematically offset by a large fraction of the formal error. Such an offset would bias the inferred orbital parameters and companion masses. This risk can be mitigated by using `htof` with the built-in ad-hoc correction.

The data corruption likewise has affected nearly the same subset of sources of the IAD on the *Hipparcos* 2007 DVD. In principle, the same ad-hoc correction is possible. However, in practice it requires substantially more computation time, because rejected transits (those marked with negative uncertainties in the Java tool) are not clearly indicated in the DVD IAD. Even the information about the number of rejected observations in the IAD header only gives the integer part of the percentage of rejected observations. This means that it is not clearly indicated if any source with less than 100 observations has zero or one rejected observation. We recommend that any work using the IAD from the *Hipparcos* 2007 DVD should exclude sources where the chi-squared partials of the data do not sum to zero. The DVD sources that `htof` failed to refit are given in `htof/data/hip2.DVD_flagged.txt`. We defined a refit failure as one with proper motion refit discrepancies exceeding 0.03 mas/yr. These stars also have significantly nonzero sums of  $\chi^2$  partials. We encourage the reader to consider using the IAD corresponding to the Java tool, where `htof` has automatic correction built-in and so these data are ready for a variety of use cases like orbit fitting.

## 5. USE CASE I: ORBIT FITTING

`htof`'s primary use case to-date is in orbit fits that incorporate *Gaia* and *Hipparcos* absolute astrometry. `htof` is implemented in `orvara` (Brandt et al. 2021d), a Markov-Chain-Monte-Carlo (MCMC) code that employs the parallel-tempering sampler `ptemcee` (Foreman-Mackey et al. 2013; Vousden et al. 2016). `htof` is used to forward model the absolute astrometry within `orvara`. `htof` and `orvara` were used, for example, to infer a precise mass for Gl 229 B (Brandt et al. 2019; Brandt et al. 2021c); produce masses and orbital parameters for two white dwarf companions (Bowler



et al. 2021a); yield a dynamical mass estimate for a newly discovered brown dwarf companion to HD 33632 (Currie et al. 2020); infer the mass of a substellar companion to HD 47127 (Bowler et al. 2021b); produce refined masses and orbital parameters for  $\beta$  Pic b and c (Brandt et al. 2021a); derive the first dynamical mass for HR 8799 e (Brandt et al. 2021b); derive precise masses for six directly imaged brown dwarfs (Brandt et al. 2021c); and solve for masses (breaking the inclination degeneracy) of nine massive companions that previously had only RV detections (Li et al. 2021).

`htof` uses the *Gaia* scanning law, *Hipparcos* 1997 and 2007 IAD to forward model perturbations to the absolute astrometry due to companions. `htof` computes three proper motion perturbations per MCMC step: one for *Gaia*, one for *Hipparcos*, and finally one to the HGCA long-baseline proper motion. The unperturbed proper motions are cross-calibrated and have already been placed in a common reference frame (Brandt 2018, 2021). `htof`'s forward modelling of the absolute astrometry is particularly relevant for sources where the precision on the mass of the companion is high. For Gl 229 B, with a mass measured to  $\lesssim 1\%$ , disabling `htof`'s exact forward modelling causes the inferred mass of the companion to shift by an amount comparable to its formal uncertainty (Brandt et al. 2021c).

## 6. USE CASE II: ASTROMETRIC MISSION FORECASTING

Precision astrometric missions can detect and characterize companions around stars by observing the reflex motion of the star in the plane of the sky due to its companion. *Gaia* expects to detect tens of thousands of sub-stellar companions over its nominal 5-year mission (Perryman et al. 2014). However, many additional missions have been proposed (in part) for exoplanet discovery and characterization. For example SIM and SIM Lite (which aimed at roughly  $\mu\text{as}$  precision; Unwin et al. 2008; Shao et al. 2009), JASMINE (formerly named Small-JASMINE;<sup>11</sup> Gouda 2019), TOLIMAN (Delli Veneri et al. 2021), Theia (The Theia Collaboration et al. 2017; Malbet et al. 2019), and *NGRST* (Spergel et al. 2015; Melchior et al. 2018). Here we show how `htof` can calculate new planets that would be discoverable in the  $\beta$  Pic system if one combined *Hipparcos*, *Gaia* and *NGRST* measurements. The example discussed in this section is contained in the Jupyter examples notebook that accompanies `htof`. `htof`'s mission

forecasting capability is applicable to any combination of astrometric missions for any star.

### 6.1. Data and assumptions

For *NGRST*, we use the  $10\mu\text{as}$  precision estimated by Sanderson et al. (2017) for spatial scanning (single scan). Melchior et al. (2018) estimate a  $\sim 10\mu\text{as}$  precision for bright stars from centering on diffraction spikes. The end-of-mission performance of *Gaia* on bright stars is expected to be a factor of a few better than it is in EDR3. The exact end-of-mission single-scan precision for *Gaia* is unavailable but we estimate it as follows. The *Gaia* collaboration predicts  $10\mu\text{as}$  parallax precision by *Gaia* DR4 for bright stars ( $3 < V < 12$ ).<sup>12</sup> The error on the sky-averaged position is  $0.75 \times$  the parallax precision. Each source will be observed  $\sim 100$  times. A rough estimate of the single-exposure precision is then  $\sim 10 \cdot 0.75 \sqrt{100} \mu\text{as} = 75 \mu\text{as}$ . We inflate this slightly, to be conservative, to  $120 \mu\text{as}$ .

We now consider which planets are detectable given three different combinations of data on  $\beta$  Pic: *Gaia* alone (which we label as *Gaia*), *Gaia* combined with *Hipparcos* (*Gaia*+HIP), and *Gaia* combined with a mock *NGRST* campaign (*Gaia*+*NGRST*). The mock *NGRST* campaign of  $\beta$  Pic consists of six randomly spaced *NGRST* spatial-scanning observations between 2025 and 2028. We assume a diagonal covariance matrix for each *NGRST* observation with  $10\mu\text{as}$  errors in right-ascension and declination. The mock *Gaia* DR4 data are the 91 *Gaia* GOST observations planned for  $\beta$  Pic between 2014 and 2020. We assume equal along-scan errors of  $120\mu\text{as}$  and zero covariance between measurements. The *Hipparcos* data we use are the actual *Hipparcos* observations of  $\beta$  Pic from the 1997 reduction IAD.

We compute the  $\Delta\chi^2$  of a linear astrometric fit to the perturbed motion of  $\beta$  Pic for a swath of planetary masses and semi-major axes. For any given mass and semi-major axis, we assume a circular edge-on orbit ( $i = 90^\circ$ ) around  $\beta$  Pic A. We assume that effects like apparent acceleration from projected linear motion and timing fluctuations from light travel time have been accounted for. Finally, we take the average  $\Delta\chi^2$  across a uniform distribution of orbital phases. We define a body as detectable if it causes an astrometric perturbation on its host star with  $\Delta\chi^2 > 30$  where  $\Delta\chi^2 = 0$  implies linear motion perfectly described by five astrometric parameters.  $\Delta\chi^2 > 30$  is the ‘marginal’ detection criterion from Perryman et al. (2014).  $\Delta\chi^2 > 100$

<sup>11</sup> <http://jasmine.nao.ac.jp/index-en.html> and <http://www.scholarpedia.org/article/JASMINE>

<sup>12</sup> <https://www.cosmos.esa.int/web/gaia/science-performance>

is a strong detection where orbital parameters can typically be constrained to better than 10% (Perryman et al. 2014).

### 6.2. Results and discussion

Figure 3 shows the parameter space of hypothetical planets around  $\beta$  Pic A that are detectable. The known planets  $\beta$  Pic b and  $\beta$  Pic c are shown. We show contours of  $\Delta\chi^2 > 30$  in mass and semi-major axis space for  $\beta$  Pic for all three cases: *Gaia*, *Gaia*+*NGRST*, and *Gaia*+*HIP*. *Hipparcos* will be important for potential short-period planets in  $\beta$  Pic only if the *Gaia* end-of-mission parallax precision is substantially worse than  $16 \mu\text{as}$ . In the *Gaia*+*NGRST* case (all blue regions), adding *Hipparcos* astrometry negligibly enlarges the detectable region because of the already long time baseline between *Gaia* and *NGRST* and the high precision of *NGRST*.  $\beta$  Pic c is detectable with confidence with *Gaia* DR4 alone ( $\Delta\chi^2$  exceeds 400) and with extreme confidence ( $\Delta\chi^2$  exceeds 1000) if combined with six *NGRST* observations. An unseen Saturn mass companion could be detected by combining *Gaia* and *NGRST*.

Lagrange et al. (2020) ruled out the presence of additional planets in the  $\beta$  Pic system more massive than  $\sim 2.5 M_{\text{Jup}}$  closer than 3 au;  $3.5 M_{\text{Jup}}$  for planets whose semi major axis' are between 3 au and 7.5 au; and  $\sim 1\text{--}2 M_{\text{Jup}}$  for planets lying beyond 7.5 au. Figure 3 shows these limits as red lines. We find that a *Gaia* DR4 and *Hipparcos* merger could improve the limit between 3 au and 7.5 au to exclude additional planets (in edge-on orbits) more massive than  $1.5 M_{\text{Jup}}$ . Adding six *NGRST* observations could exclude edge-on planets more massive than  $0.2 M_{\text{Jup}}$ .

## 7. SUMMARY AND CONCLUSIONS

We present *htof*, an open-source tool for using the *Hipparcos* and *Gaia* astrometry in a variety of applications. *htof* provides routines to parse and fit the intermediate astrometric data from both *Hipparcos* reductions and the *Gaia* scanning law. It is prepared for future *Gaia* data releases which will include the intermediate astrometric data and higher-order fits.

We suggest that 6617 sources within *Hipparcos* 2007 have corrupted IAD, and present *htof*'s ad-hoc correction to this corruption (for the Java tool version of the IAD). *htof* can be used to forecast future astrometric missions. We find that *Gaia* DR4 merged with *Hipparcos* could improve the Lagrange et al. (2020)  $\beta$  Pic companion limits by a factor of 2, excluding additional planets more massive than  $\sim 1.5 M_{\text{Jup}}$  with semi-major axis' between 3 au and 7.5 au. Jupiter and Saturn mass companions would be astrometrically detectable around

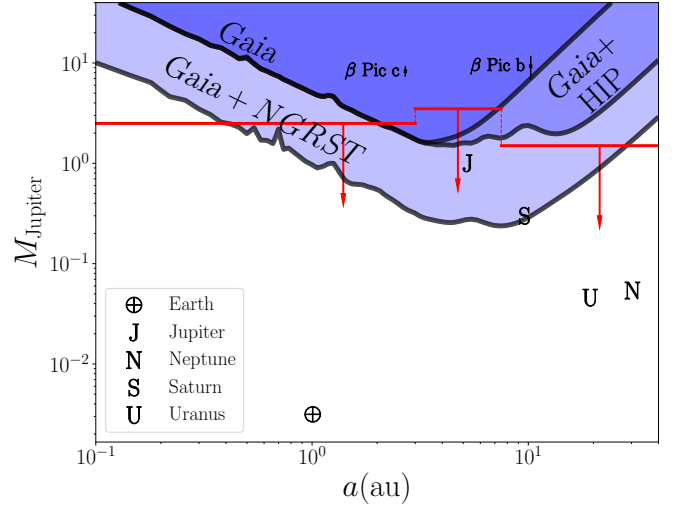


**Figure 3.** Mass and semimajor axis space for planets orbiting the star  $\beta$  Pic A in circular, edge-on orbits. Planets  $\beta$  Pic b and  $\beta$  Pic c have been placed according to their semi-major axis' and masses (Brandt et al. 2021a). Solar system planets are shown for comparison. Blue regions indicate parameter space where a planet would be detectable with  $\Delta\chi^2 > 30$  — corresponding to the Perryman et al. (2014) detection criterion. Planets in any blue region (above the *Gaia*+*NGRST* contour) would be detectable by combining *Gaia* DR4 with six *NGRST* observations. Planets in the dark-blue region above the *Gaia* contour would be detectable by *Gaia* alone, and planets in either of the darkest two regions (*Gaia* or *Gaia*+*HIP*) could be discovered through a merging of the *Gaia* and *Hipparcos* IAD. The regions above the red lines correspond to additional planets ruled out by Lagrange et al. (2020). The code to reproduce the *Gaia*+*NGRST* contour is in the Jupyter examples notebook that accompanies *htof*.

$\beta$  Pic if one combined *Gaia* DR4 with six *NGRST* observations.

*htof* is available at <https://github.com/gmbrandt/htof> and installable with `pip install htof`. The `examples.ipynb` Jupyter notebook provides examples of using *htof*. We welcome feedback and contributions.

## ACKNOWLEDGEMENTS

We thank the referee for helpful feedback on this work. We thank Anthony G. A. Brown for helpful discussions about *Gaia* and *Hipparcos*, and for the sky path module in *htof* which we obtained, with his permission, from his package *astrometric-sky-path*<sup>13</sup>. We thank Floor van Leeuwen, for supporting us with access to the IAD from the Java tool, for helping us interpret the Java tool IAD and some of their detailed properties, and for

<sup>13</sup> <https://github.com/agabrown/astrometric-sky-path>

helpful discussions of the manuscript. G. M. B. thanks Lachlan T. Lancaster for helpful discussions.

D. M. gratefully acknowledges support from the European Space Agency (ESA) Research Fellow programme. G. M. B. is supported by the National Science Foundation (NSF) Graduate Research Fellowship under grant no. 1650114.

This work made use of the REBOUND code which is freely available at <http://github.com/hannorein/rebound>. This work has made use of data from the European Space Agency (ESA) mission *Gaia* (<https://www.cosmos.esa.int/Gaia>), processed by the *Gaia* Data Processing and Analysis Consortium (DPAC, <https://www.cosmos.esa.int/web/Gaia/dpac/consortium>). Funding for the DPAC has been provided by national institutions, in particular the institutions participating in the *Gaia* Multilateral Agreement.

*Software:* astropy (Astropy Collaboration et al. 2013; Price-Whelan et al. 2018), scipy (Virtanen et al. 2020), numpy (Oliphant 2006; van der Walt et al. 2011), pandas (Wes McKinney 2010; pandas development team 2020), Jupyter,

astropy (Astropy Collaboration et al. 2013; Price-Whelan et al. 2018), scipy (Virtanen et al. 2020), numpy (Oliphant 2006; van der Walt et al. 2011), pandas (Wes McKinney 2010; pandas development team 2020), Jupyter,

## APPENDIX

### A. THE AD-HOC CORRECTION ALGORITHM

Here we detail the ad-hoc correction algorithm for the *Hipparcos* 2007 Java tool IAD. The Jupyter notebook with the source code contains examples that demonstrate the ad-hoc correction.

1. We separate the IAD into two blocks: the first five columns (orbit number, epoch, parallax factor, sine and cosine of the scan angle) into the left-hand side block L; and the last two columns (residuals and AL errors) into the right-hand side block R.
2. We assume that the last  $n$  residuals and (typically duplicate) along-scan errors are corrupted and therefore remove the last  $n$  rows from block R. This results in  $n$  too many rows in block L.
3. We iterate through all possible combinations of removing  $n$  rows from block L.<sup>14</sup> For each iteration:
  - (a) Blocks L and R now have the same number of rows again. We recombine blocks L and R, yielding a modified IAD.
  - (b) We calculate the quadrature sum of the chi-squared partials for this modified IAD.
4. We accept the modified IAD that gives the smallest quadrature sum of the chi-squared partials. This sum is typically less than 0.01.

## REFERENCES

- Astropy Collaboration, Robitaille, T. P., Tollerud, E. J., et al. 2013, *A&A*, 558, A33, doi: [10.1051/0004-6361/201322068](https://doi.org/10.1051/0004-6361/201322068)
- Bowler, B. P., Cochran, W. D., Endl, M., et al. 2021a, *AJ*, 161, 106, doi: [10.3847/1538-3881/abd243](https://doi.org/10.3847/1538-3881/abd243)
- Bowler, B. P., Endl, M., Cochran, W. D., et al. 2021b, arXiv e-prints, arXiv:2105.01255. <https://arxiv.org/abs/2105.01255>
- Brandt, G. M., Brandt, T. D., Dupuy, T. J., Li, Y., & Michalik, D. 2021a, *AJ*, 161, 179, doi: [10.3847/1538-3881/abdc2e](https://doi.org/10.3847/1538-3881/abdc2e)
- Brandt, G. M., Brandt, T. D., Dupuy, T. J., Michalik, D., & Marleau, G.-D. 2021b, *ApJL*, 915, L16, doi: [10.3847/2041-8213/ac0540](https://doi.org/10.3847/2041-8213/ac0540)
- Brandt, G. M., & Michalik, D. 2021, *HTOF*, 1.0.0, Zenodo, doi: [10.5281/zenodo.5495866](https://doi.org/10.5281/zenodo.5495866)
- Brandt, G. M., Dupuy, T. J., Li, Y., et al. 2021c, arXiv e-prints, arXiv:2109.07525. <https://arxiv.org/abs/2109.07525>
- Brandt, T. D. 2018, *The Astrophysical Journal Supplement Series*, 239, 31, doi: [10.3847/1538-4365/aaec06](https://doi.org/10.3847/1538-4365/aaec06)
- . 2021, arXiv e-prints, arXiv:2105.11662. <https://arxiv.org/abs/2105.11662>
- Brandt, T. D., Dupuy, T. J., & Bowler, B. P. 2018, arXiv e-prints, arXiv:1811.07285. <https://arxiv.org/abs/1811.07285>
- Brandt, T. D., Dupuy, T. J., Bowler, B. P., et al. 2019, *A Dynamical Mass of  $70 \pm 5$  Jupiter Masses for Gliese 229B, the First Imaged T Dwarf*. <https://arxiv.org/abs/1910.01652>

<sup>14</sup> We speed up the algorithm for the 180 sources with  $n \geq 5$ . These have a large number of combinatoric possibilities. Often, one orbit contains multiple observations. These often almost have identical epochs and scan angles. For all practical purposes, we find that it does not matter which one of the observations within one orbit we remove, as long as we remove the correct number of observations from that orbit.

- Brandt, T. D., Dupuy, T. J., Li, Y., et al. 2021d, arXiv e-prints, arXiv:2105.11671.  
<https://arxiv.org/abs/2105.11671>
- Calissendorff, P., & Janson, M. 2018, ArXiv e-prints.  
<https://arxiv.org/abs/1806.07899>
- Currie, T., Brandt, T. D., Kuzuhara, M., et al. 2020, ApJL, 904, L25, doi: [10.3847/2041-8213/abc631](https://doi.org/10.3847/2041-8213/abc631)
- de Bruijne, J. H. J., & Eilers, A.-C. 2012, A&A, 546, A61, doi: [10.1051/0004-6361/201219219](https://doi.org/10.1051/0004-6361/201219219)
- De Rosa, R. J., Dawson, R., & Nielsen, E. L. 2020, A&A, 640, A73, doi: [10.1051/0004-6361/202038496](https://doi.org/10.1051/0004-6361/202038496)
- Delli Veneri, M., Desdoigts, L., Schmitz, M. A., et al. 2021, Periodic Astrometric Signal Recovery Through Convolutional Autoencoders, Vol. 39, 167–195, doi: [10.1007/978-3-030-65867-0\\_8](https://doi.org/10.1007/978-3-030-65867-0_8)
- Dupuy, T. J., Brandt, T. D., Kratter, K. M., & Bowler, B. P. 2019, ApJL, 871, L4, doi: [10.3847/2041-8213/aafb31](https://doi.org/10.3847/2041-8213/aafb31)
- ESA. accessed February 4, 2020,  
<https://www.cosmos.esa.int/web/gaia/scanning-law>
- Feng, F., Anglada-Escudé, G., Tuomi, M., et al. 2019, MNRAS, 490, 5002, doi: [10.1093/mnras/stz2912](https://doi.org/10.1093/mnras/stz2912)
- Fernández-Hernández, J., & Joliet, E. 2019, GOST Software User Manual, Gaia DPAC
- Fontanive, C., Mužić, K., Bonavita, M., & Biller, B. 2019, MNRAS, 490, 1120, doi: [10.1093/mnras/stz2587](https://doi.org/10.1093/mnras/stz2587)
- Foreman-Mackey, D., Hogg, D. W., Lang, D., & Goodman, J. 2013, PASP, 125, 306, doi: [10.1086/670067](https://doi.org/10.1086/670067)
- Gaia Collaboration, Brown, A. G. A., Vallenari, A., et al. 2020, arXiv e-prints, arXiv:2012.01533.  
<https://arxiv.org/abs/2012.01533>
- Gaia Collaboration, Prusti, T., de Bruijne, J. H. J., et al. 2016, A&A, 595, A1, doi: [10.1051/0004-6361/201629272](https://doi.org/10.1051/0004-6361/201629272)
- Gaia Collaboration, Brown, A. G. A., Vallenari, A., et al. 2018a, A&A, 616, A1, doi: [10.1051/0004-6361/201833051](https://doi.org/10.1051/0004-6361/201833051)
- Gaia Collaboration, Spoto, F., Tanga, P., et al. 2018b, A&A, 616, A13, doi: [10.1051/0004-6361/201832900](https://doi.org/10.1051/0004-6361/201832900)
- Gouda, N. 2019, Proceedings of the International Astronomical Union, 14, 51–53, doi: [10.1017/S17439213190007968](https://doi.org/10.1017/S17439213190007968)
- Kervella, P., Arenou, F., Mignard, F., & Thévenin, F. 2019, A&A, 623, A72, doi: [10.1051/0004-6361/201834371](https://doi.org/10.1051/0004-6361/201834371)
- Lagrange, A. M., Rubini, P., Nowak, M., et al. 2020, A&A, 642, A18, doi: [10.1051/0004-6361/202038823](https://doi.org/10.1051/0004-6361/202038823)
- Li, Y., Brandt, T. D., Brandt, G. M., et al. 2021, arXiv e-prints, arXiv:2109.10422.  
<https://arxiv.org/abs/2109.10422>
- Lindgren, L., & Dravins, D. 2021, arXiv e-prints, arXiv:2105.09014. <https://arxiv.org/abs/2105.09014>
- Lindgren, L., Mignard, F., Söderhjelm, S., et al. 1997, A&A, 323, L53
- Lindgren, L., Hernandez, J., Bombrun, A., et al. 2018, arXiv. <https://arxiv.org/abs/1804.09366>
- Lindgren, L., Klioner, S. A., Hernández, J., et al. 2020, arXiv e-prints, arXiv:2012.03380.  
<https://arxiv.org/abs/2012.03380>
- Luyten, W. J. 1979, LHS catalogue. A catalogue of stars with proper motions exceeding 0"5 annually
- Maire, A. L., Molaverdikhani, K., Desidera, S., et al. 2020, A&A, 639, A47, doi: [10.1051/0004-6361/202037984](https://doi.org/10.1051/0004-6361/202037984)
- Malbet, F., Abbas, U., Alves, J., et al. 2019, arXiv e-prints, arXiv:1910.08028. <https://arxiv.org/abs/1910.08028>
- Melchior, P., Spergel, D., & Lanz, A. 2018, AJ, 155, 102, doi: [10.3847/1538-3881/aaa422](https://doi.org/10.3847/1538-3881/aaa422)
- Michalik, D., Lindgren, L., Hobbs, D., & Lammers, U. 2014, A&A, 571, A85, doi: [10.1051/0004-6361/201424606](https://doi.org/10.1051/0004-6361/201424606)
- Nielsen, E. L., De Rosa, R. J., Wang, J. J., et al. 2019, arXiv e-prints, arXiv:1911.11273.  
<https://arxiv.org/abs/1911.11273>
- Oliphant, T. 2006, NumPy: A guide to NumPy, USA: Trelgol Publishing. <http://www.numpy.org/>
- pandas development team, T. 2020, pandas-dev/pandas: Pandas, 1.0.5, Zenodo, doi: [10.5281/zenodo.3509134](https://doi.org/10.5281/zenodo.3509134)
- Perryman, M. 2012, European Physical Journal H, 37, 745, doi: [10.1140/epjh/e2012-30039-4](https://doi.org/10.1140/epjh/e2012-30039-4)
- Perryman, M., Hartman, J., Bakos, G. Á., & Lindgren, L. 2014, ApJ, 797, 14, doi: [10.1088/0004-637X/797/1/14](https://doi.org/10.1088/0004-637X/797/1/14)
- Perryman, M. A. C., Lindgren, L., Kovalevsky, J., et al. 1997, A&A, 500, 501
- Price-Whelan, A. M., Sipőcz, B. M., Günther, H. M., et al. 2018, AJ, 156, 123, doi: [10.3847/1538-3881/aabc4f](https://doi.org/10.3847/1538-3881/aabc4f)
- Quirrenbach, A., Reffert, S., & Bergmann, C. 2011, in American Institute of Physics Conference Series, Vol. 1331, Planetary Systems Beyond the Main Sequence, ed. S. Schuh, H. Drechsel, & U. Heber, 102–109, doi: [10.1063/1.3556189](https://doi.org/10.1063/1.3556189)
- Reffert, S., & Quirrenbach, A. 2011, A&A, 527, A140, doi: [10.1051/0004-6361/201015861](https://doi.org/10.1051/0004-6361/201015861)
- Sahlmann, J., Ségransan, D., Queloz, D., et al. 2011, A&A, 525, A95, doi: [10.1051/0004-6361/201015427](https://doi.org/10.1051/0004-6361/201015427)
- Sanderson, R. E., Bellini, A., Casertano, S., et al. 2017, arXiv e-prints, arXiv:1712.05420.  
<https://arxiv.org/abs/1712.05420>
- Shao, M., Marcy, G., Catanzarite, J. H., et al. 2009, in astro2010: The Astronomy and Astrophysics Decadal Survey, Vol. 2010, 271. <https://arxiv.org/abs/0904.0965>
- Snellen, I. A. G., & Brown, A. G. A. 2018, Nature Astronomy, 2, 883, doi: [10.1038/s41550-018-0561-6](https://doi.org/10.1038/s41550-018-0561-6)



- Sozzetti, A., & Desidera, S. 2010, *A&A*, 509, A103, doi: [10.1051/0004-6361/200912717](https://doi.org/10.1051/0004-6361/200912717)
- Spergel, D., Gehrels, N., Baltay, C., et al. 2015, arXiv e-prints, arXiv:1503.03757.  
<https://arxiv.org/abs/1503.03757>
- The Theia Collaboration, Boehm, C., Krone-Martins, A., et al. 2017, arXiv e-prints, arXiv:1707.01348.  
<https://arxiv.org/abs/1707.01348>
- Unwin, S. C., Shao, M., Tanner, A. M., et al. 2008, *PASP*, 120, 38, doi: [10.1086/525059](https://doi.org/10.1086/525059)
- van de Kamp, P. 1935, *AJ*, 44, 74, doi: [10.1086/105263](https://doi.org/10.1086/105263)
- van der Walt, S., Colbert, S. C., & Varoquaux, G. 2011, *Computing in Science and Engineering*, 13, 22, doi: [10.1109/MCSE.2011.37](https://doi.org/10.1109/MCSE.2011.37)
- van Leeuwen, F. 2007a, *A&A*, 474, 653, doi: [10.1051/0004-6361:20078357](https://doi.org/10.1051/0004-6361:20078357)
- . 2007b, *Hipparcos, the New Reduction of the Raw Data*, Vol. 350, doi: [10.1007/978-1-4020-6342-8](https://doi.org/10.1007/978-1-4020-6342-8)
- van Leeuwen, F., & Evans, D. W. 1998, *Astronomy and Astrophysics Supplement Series*, 130, 157, doi: [10.1051/aas:1998218](https://doi.org/10.1051/aas:1998218)
- van Leeuwen, F., & Michalik, D. 2019, Private Communication
- van Leeuwen, F., & Michalik, D. 2021, Private Communication
- Venner, A., Vanderburg, A., & Pearce, L. A. 2021, arXiv e-prints, arXiv:2104.13941.  
<https://arxiv.org/abs/2104.13941>
- Virtanen, P., Gommers, R., Oliphant, T. E., et al. 2020, *Nature Methods*, 17, 261, doi: <https://doi.org/10.1038/s41592-019-0686-2>
- Vousden, W. D., Farr, W. M., & Mandel, I. 2016, *MNRAS*, 455, 1919, doi: [10.1093/mnras/stv2422](https://doi.org/10.1093/mnras/stv2422)
- Wes McKinney. 2010, in *Proceedings of the 9th Python in Science Conference*, ed. Stéfan van der Walt & Jarrod Millman, 56 – 61, doi: [10.25080/Majora-92bf1922-00a](https://doi.org/10.25080/Majora-92bf1922-00a)
- Zucker, S., & Mazeh, T. 2001, *ApJ*, 562, 549, doi: [10.1086/322959](https://doi.org/10.1086/322959)